ACOUSTICAL LETTER

Temperature-independent fiber Bragg grating underwater acoustic sensor array using incoherent light

Satoshi Tanaka*, Hiroki Yokosuka and Nobuaki Takahashi

Department of Communications Engineering, National Defense Academy, Hashirimizu 1–10–20, Yokosuka, 239–8686 Japan

(*Received 5 April 2005, Accepted for publication 21 June 2005*)

Keywords: Acoustic sensor, Optical fiber sensor, Fiber Bragg grating, Optical switch, Time-division multiplexing
PACS number: 43.69.Qv, 43.28.We [DOI: 10.1250/ast.27.50]

1. Introduction

Recently, fiber Bragg grating (FBG) sensors have attracted considerable attention because of their practical advantages, namely, compactness, simple structure, localized sensing capability, and ease in multiplexed operation. The principles of operation in most FBG sensors are based on the change in the Bragg wavelength (λ_B) of the FBG used; the FBG is subjected to various factors [1,2], such as temperature, static strain, mechanical vibration, hydrostatic pressure, acoustic wave, and so forth. We previously demonstrated several methods of fabricating FBG vibration sensors with a temperature-independent operation [3–5]. In this study, an FBG underwater acoustic sensor is proposed. In addition, a sensor scheme is developed to construct a sensor array from a practical viewpoint. In an experiment, by constructing an FBG underwater acoustic sensor array in which two sensor elements are arranged in parallel, time-division multiplexed detection and temperature-insensitive operation are demonstrated.

2. Principle of operation

Figure 1 shows a schematic configuration of a reflective FBG underwater acoustic sensor. This sensor uses a broadband light source such as an amplified spontaneous emission (ASE) source and consists of a four-port optical circulator and a pair of FBGs, namely, FBG_L and FBG_S, which are used as a light source and a sensing component, respectively. As shown on the right-hand side of Fig. 1, the spectral bandwidth of FBG_L is relatively narrower than that of FBG_S, and its peak wavelength, i.e., the Bragg wavelength λ_{BL}, is set to the slope of the transmission spectrum curve of FBG_S. The four-port optical circulator transmits the incident light from port 1, 2, or 3 to port 2, 3, or 4, respectively. As a result, the broadband light from port 2 is reflected at FBG_L, and the reflected light is incident on FBG_S, serving as a narrowband optical source of the FBG sensor. Consequently, the output signal light, i.e., the light transmitted by FBG_S, is coupled back from port 2 of the circulator. In this situation, when an acoustic wave is applied to FBG_S, the transmission spectrum of FBG_S shifts periodically in a wavelength domain so that its transmitted light intensity is modulated. At the photodetector, the acoustic wave can be directly observed from the ac component of the detected output signal from the sensor. It should be noted here that the sensitivity of the sensor output is defined by the gradient at the slope of the transmission spectrum curve of FBG_S. In addition, the effects of temperature on the sensor output can be compensated using the pair of FBGs; if FBG_L is subjected to the environmental temperature change equal to that around FBG_S, the relative spectral position between the narrowband optical source and transmission spectrum curve of the sensing FBG is maintained constant in the wavelength domain. On the other hand, the acoustic effects toward FBG_L are almost inhibited by the shielding aluminum tube filled with air at FBG_L, achieving the acoustic detection with the temperature-independent operation. In addition, the single lead-in/out fiber of the sensor enables us to form an arrayed sensor arrangement with a single optical light source and a single receiving photodetector.

3. Experiment

Figure 2 shows the experimental setup of the FBG underwater acoustic sensor array. Here, two sensors, sensors 1 and 2, were multiplexed using a two-channel optical switch. For an experimental demonstration of underwater acoustic detection, both the sensors were immersed in water vessels, WV_1 and WV_2, respectively, and acoustic waves were applied independently to the sensors using piezoelectric transducers (PZT_1 and PZT_2). The intensity-modulated signals, i.e., the outputs from the elements of the sensor array, are extracted

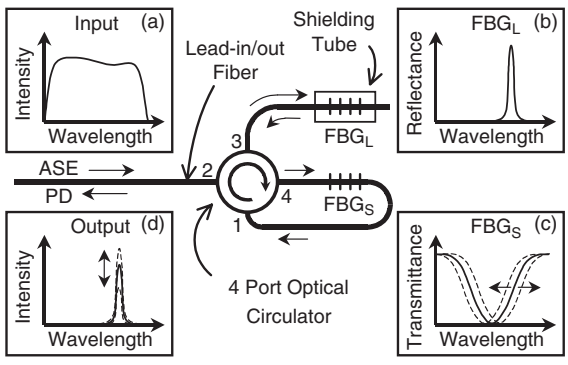

Fig. 1 Schematic configuration of reflective FBG underwater acoustic sensor: (a) input spectrum of incoherent light source, (b) reflection spectrum of FBG for light source, (c) transmission spectrum of FBG for sensor, and (d) output spectrum of intensity-modulated light from FBG.

*e-mail: satoshi@nda.ac.jp

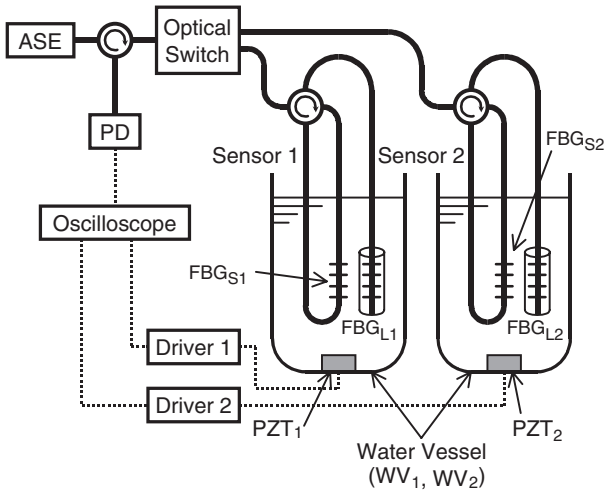

Fig. 2 Experimental setup.

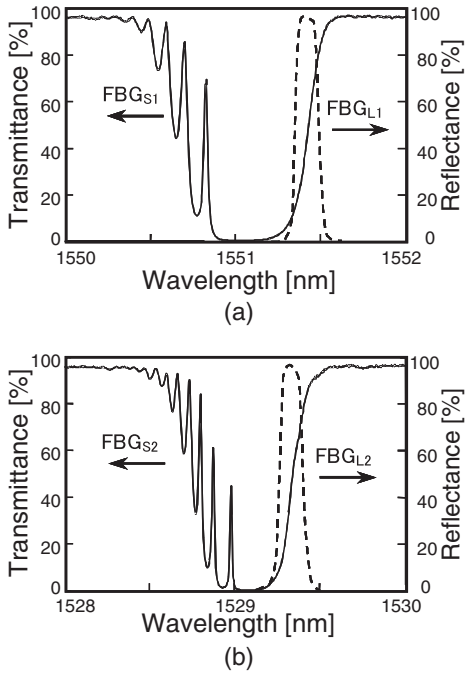

Fig. 3 Transmission spectra of FBGs for sensing elements (solid lines) together with reflection spectra of FBG for light sources (dashed lines). The reflectance of FBG_{L1} and transmittance of FBG_{S1} are shown in (a), and the reflectance of FBG_{L2} and transmittance of FBG_{S2}, in (b).

from the photodetector PD, and the optical switch enables us to detect time-division multiplexed sensor outputs. In the experiment, we used specially designed FBGs to form the FBG underwater acoustic sensor array. The reflection and transmission spectra of the FBGs measured at room temperature are shown in Fig. 3: the reflectance of FBG_{L1} and transmittance of FBG_{S1} are shown in Fig. 3(a), and the reflectance of FBG_{L2} and transmittance of FBG_{S2} in Fig. 3(b). In these figures, the dashed and solid curves denote, respectively, the reflection and transmission spectrum curves. As

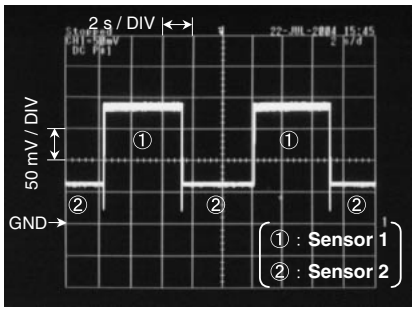

Fig. 4 Typical sensor outputs from photodetector PD. The trace signals shown in ① and ② denote the outputs from sensors 1 and 2, respectively.

can be seen from the figures, the respective peak wavelength of the reflection spectrum of FBG_{L1} or FBG_{L2}, i.e., λ_{BL1} or λ_{BL2}, is set to the slope of the respective transmission spectrum of FBG_{S1} or FBG_{S2}.

4. Results and discussion

To demonstrate the underwater acoustic detection of the FBG sensor array, acoustic waves were induced in both the water vessels using cylindrical PZTs. The PZTs were driven in the sinusoidal mode and their driving frequencies were 16.6 and 17.0 kHz, which correspond to their resonance frequencies. The detected signal at the photodetector PD was fed into an oscilloscope and monitored, while the channel of the optical switch was changed periodically with an interval of 5 s. The trace of the signal obtained from PD is shown in Fig. 4. As shown in the figure, when sensor 1 is selected using the optical switch, the output signal due to the acoustic wave in the water vessel (WV_1) is detected at PD (①), while the output signal due to the acoustic wave in WV_2 is obtained with sensor 2 (②). The expanded trace signals of the ac components of the obtained output signals for sensors 1 and 2 are represented in Figs. 5(a) and 5(b), respectively. Since the waveform distortions of both the signals are small, it is expected that the sensor outputs will result in a linear response. Figure 6 shows the measured output of sensor 1 as a function of the amplitude of the applied voltage to PZT_1 and the corresponding sound pressure level. To monitor the sound pressure level around the sensor, an electrical hydrophone was used as a reference. As can be seen from the figure, the obtained result shows a good linear response against the applied acoustic wave.

To examine the temperature-independent operation in underwater acoustic detection, the output of sensor 1 was monitored as a function of environmental temperature, while keeping the sound pressure level around the sensor and the frequency of PZT_1 constant; however, the temperature of the water was varied between 27 and 75°C. The plots with solid squares show the sensor outputs when the sensor is not thermally stabilized, in which only FBG_{S1} is immersed in WV_1, whereas FBG_{L1} is removed from WV_1 in order to keep its temperature constant (27°C). The plots with solid circles show the sensor outputs when both FBG_{L1} and FBG_{S1} are immersed in WV_1 so that common temperature variations are applied to the FBGs, i.e., the sensor is operated in the temperature-independent mode. It is noted that the sensor

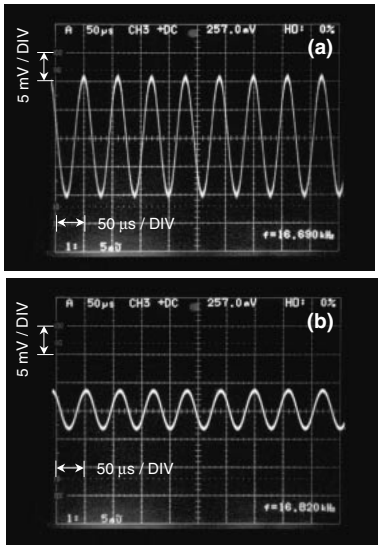

Fig. 5 Expanded representation of ac components of sensor outputs from sensors 1 (a) and 2 (b).

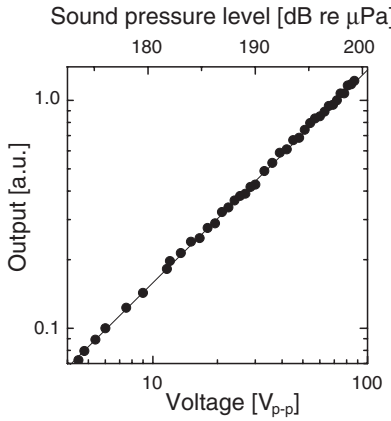

Fig. 6 Dependences of sensor output from sensor 1 on acoustic pressure and voltage applied to transducer used.

output without the temperature-independent operation varies considerably. The minimum sensor output of approximately −68 dB corresponds to the noise level of the detected signal. The output variation of the sensor without temperature stabilization was estimated to be more than 35 dB. On the other hand, with the stabilization, the output variation of the sensor was estimated to be less than 3 dB.

5. Conclusion

A reflective fiber Bragg grating (FBG) sensor was developed to construct an FBG underwater acoustic sensor array, which consists of a broadband ASE source, a four-port optical circulator and a pair of FBGs: one is used for acoustic sensing, and the other is used to provide a narrowband light source from the ASE source. In this arrangement, the temperature-dependent output variation of the sensor can be eliminated when common temperature changes are applied to the pair of FBGs. In addition, the sensor uses a single lead-in/out fiber so that it is convenient to apply this type of sensor to the elements of a sensor array. To confirm the operational principle of the sensor array proposed, two FBG sensor elements were fabricated and an underwater acoustic sensor array was constructed using an optical switch. In the experiment, time-division multiplexed multiple acoustic detection and temperature-insensitive operation were successfully demonstrated. The output variation without temperature stabilization was estimated to be more than 35 dB, whereas that with the stabilization was estimated to be less than 3 dB.

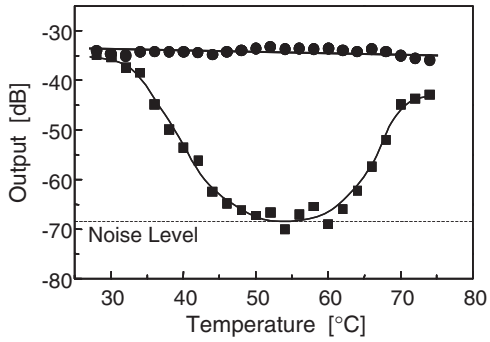

Fig. 7 Temperature-dependent sensor outputs: with (solid circles) and without (solid squares) temperature compensation.

References

[1] P. St. J. Russell and J. L. Archambault, *Optical Fiber Sensors* B. Culshaw and J. Dakin, Eds. (Artech House, Boston, 1996), Vol. 3, Chap. 2.

[2] A. D. Kersey, M. A. Davis, H. J. Patrik, M. LeBlanc, K. P. Koo, C. G. Askins, M. A. Putnum and E. J. Friebele, "Fiber grating sensors," *J. Lightwave Technol.*, **15**, 1442–1463 (1997).

[3] N. Takahashi, K. Yoshimura and S. Takahashi, "Fiber Bragg grating vibration sensor using incoherent light," *Jpn. J. Appl. Phys.*, **40**, 3632–3636 (2001).

[4] N. Takahashi, T. Weerapong, T. Ogawa, S. Tanaka and S. Takahashi, "Thermally stabilized fiber-Bragg-grating vibration sensor using servo motor control," *Opt. Rev.*, **10**, 106–110 (2003).

[5] S. Tanaka, T. Ogawa, T. Weerapong, N. Takahashi and S. Takahashi, "Thermally stabilized fiber-Bragg-grating vibration sensor using erbium-doped fiber laser," *Jpn. J. Appl. Phys.*, **42**, 3060–3062 (2003).